Utilization of a Very Large Mobile Offshore Structure for Clean Energy Conversion

Ken Takagi, Wataru Yano and Koichi Yamamoto

Department of Naval Architecture and Ocean Engineering, Osaka University
2-1 Yamadaoka Suita, Osaka 565-0871, Japan
Tel. +81-6-6879-7571, Fax. +81-6-6879-7594
Email: takagi@naoe.eng.osaka-u.ac.jp

***Abstract*- We proposed a new design concepts of a very large floating structure with thrusters (we call it VLMOS; Very Large Mobile Offshore Structure) that is utilized as a carrier of the renewable energy plant. In order to get good mobility, VLMOS has a configuration that a broad deck is supported by many slender lower hulls and vertical columns.**

Green function for hydroelastic analysis of vibrating free-free plates by Eatock Taylor and Ohkus is used for representing the elastic motion of the deck and the conventional modal analysis and the three-dimensional boundary element method are employed for the hydroelastic analysis of the lower hull. Some numerical results suggest that the deformation of the deck is relatively large in beam seas. A system for reducing the deformation is considered. The system reduces the deformation and generates electrical power at the same time. A two-dimensional model is used to analyze the system.

I. INTRODUCTION

Recent years are showing increasing temperatures in various regions, and/or increasing extremities in weather patterns and, many reports from various scientist show that climate change is here, and further, that human activity has contributed to it. Besides the global warming, exhaustion of the fossil fuels has been on notice since 1970s. Therefore, the renewable clean energy such as solar energy and wind energy are in the limelight recently. The solar energy and the wind energy are in practice in many countries, although their share is very small compared with fossil fuels or nuclear energy. The biggest problem on the practical application of these renewable energies in Japan is that Japan is composed of mountainous islands and has no advantage as a location of renewable energy plant. However, the EEZ (Exclusive Economic Zone) of Japan is broad and has many possibilities of utilization. We proposed a new design concept of a very large floating structure with thrusters (we call it VLMOS; Very Large Mobile Offshore Structure) that is utilized as a carrier of the renewable energy plant (see Takagi et al. [1]). It is apparent that the concept of VLMOS is suitable for the solar energy plant, because it requires a large area while Japan has no such a broad area in the country. The structure is planned to sail in the EEZ of Japan and the generated energy is transformed into hydrogen, which is easily transported by shuttle tankers.

The mobility plays an important role on this concept, since the weather condition affects a lot on the efficiency of power plants. If the structure is mobile, we could move the structure to get the maximum efficiency of the power plant. Mobility gives another benefit that the structure is free from the mooring system and also its cost. In order to get good mobility, VLMOS has a configuration that a broad deck is supported with many slender lower hulls and vertical columns. Since the section of lower hulls is semicircle for minimizing the resistance due to the surface friction, it is supposed that the wave exciting force on lower hulls is not small. Thus we need to analyze the hydroelastic behavior of VLMOS in waves for the design of a early prototype. Green function for hydroelastic analysis of vibrating free-free plates by Eatock Taylor and Ohkus [2] is used for representing the elastic motion of the deck and the conventional modal analysis and the three-dimensional boundary element method are employed for the hydroelastic analysis of the lower hull. Combining these methods, the hydroelastic behavior of VLMOS in waves is analyzed first by Takagi and Yano [3]. Some numerical results, which will be shown in the section II, suggest that the deformation of the deck is relatively large in beam seas. In order to reduce the deformation, a system, which reduces the deformation and generates electrical power at the same time, is proposed.

II. FORMULATION OF THE PROBLEM

Suppose a VLMOS which has a very large flat deck supported with $2N\times 2M$ columns and 2N slender lower hulls as shown in Fig.1. Cartesian coordinate system (x, y, z) is defined so that the z axis is vertically upward and x-y plane coincides with the calm water surface.

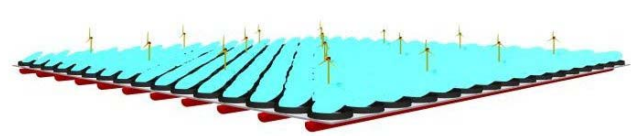

Fig.1 Image of a Very Large Mobile Offshore Structure.

The following assumptions are employed regarding the elastic behavior of the hull structure.

- The elastic behavior of the upper deck is represented by the thin elastic plate theory.
- Deformations in the x-y plane of the upper deck are represented by the two-dimensional stress field theory.
- Columns are not deformable, since they are fat and short.
- Lower hulls deflect according to the Euler beam theory in horizontal and vertical plane.

- Lower hulls are compressed or extended in the longitudinal direction.
- Lower hulls twist as a slender axisymmetry beam.

In addition to these assumptions, it is assumed that the fluid is incompressible, inviscid and irrotational. The fluid motion accords with the linear free surface and body surface condition. It is also assumed that all motions are sinusoidal in time with the circular frequency ω. The method of analysis first applied by Takagi and Yano [3]. Only the outline of the method is shown here.

A. Equation of motions

It is very important to define the elastic modes of the hull structure properly, since it strongly affects the efficiency of the computation. We assumed that the shape of VLMOS is symmetry with respect to the x-axis and y-axis. In order to reduce the computational time, we use this symmetry property.

The instantaneous shape of the n-th hull is represented as

$$b_n\left(x-\tilde{\xi}_{n,1} y - y_n - \tilde{\xi}_{n,2} + z\tilde{\xi}_{n,4}\right) - \left(y-y_n\right)\tilde{\xi}_{n,4} - z - \tilde{\xi}_{n,3} = 0, \tag{2.1}$$

where the centerline of the ***n***-th hull is located on $y=y_n$, $b_n(x,y)-z=0$ is the original n-th hull shape, $\tilde{\xi}_{n,1}(x,t)=\Re\left[\xi_{n,1}(x)\exp(i\omega t)\right]$ is telescopic deformation in the longitudinal direction, $\tilde{\xi}_{n,2}(x,t)=\Re\left[\xi_{n,2}(x)\exp(i\omega t)\right]$ is the horizontal deflection $\tilde{\xi}_{n,3}(x,t)=\Re\left[\xi_{n,3}(x)\exp(i\omega t)\right]$ is the vertical deflection and $\tilde{\xi}_{n,4}(x,t)=\Re\left[\xi_{n,4}(x)\exp(i\omega t)\right]$ is the twisting deformation.

It is assumed that the deformations of the *n*-th hull are represented by a linear combination of the vibration modes :

$$\xi_{n,1}(x)=\sum_{j=0}^{\infty}\left(X_{n,8j+1} \pm X_{n,8j+2}\right)\tilde{\psi}_{j+1}(x), \tag{2.2}$$

$$\xi_{n,2}(x)=\sum_{j=0}^{\infty}\left(\pm X_{n,8j+3} \pm X_{n,8j+4}\right)\psi_{j+1}(x), \tag{2.3}$$

$$\xi_{n,3}(x)=\sum_{j=0}^{\infty}\left(X_{n,8j+5} \pm X_{n,8j+6}\right)\psi_{j+1}(x), \tag{2.4}$$

$$\xi_{n,4}(x)=\sum_{j=0}^{\infty}\left(\pm X_{n,8j+7} + X_{n,8j+8}\right)\tilde{\psi}_{j+1}(x), \tag{2.5}$$

where $X_{n,j}$ is the amplitude of the j-th vibration mode of the n-th lower full, and we take plus sign, if $n \le N$, and we take minus sign, if $n > N$. The vibration modes are given as follows:

$$\tilde{\psi}_j(x)=\sqrt{2}\cos\frac{j-1}{L}\pi\left(x+\frac{L}{2}\right), \tag{2.6}$$

$$\psi_1(x)=1,\ \ \psi_2(x)=\sqrt{2}\,\frac{x}{L}, \tag{2.7}$$

$$\psi_j(x)=\frac{\cosh p_j L-\cos p_j L}{\sinh p_j L-\sin p_j L}\left\{\begin{array}{l}\sinh p_j\left(x+\dfrac{L}{2}\right)\\ +\sin p_j\left(x+\dfrac{L}{2}\right)\end{array}\right\} -\cosh p_j\left(x+\frac{L}{2}\right)-\cos p_j\left(x+\frac{L}{2}\right), \tag{2.8}$$

where p_j is a root of $\cos p_j L \cosh p_j L = 1$ and ***L*** is the length of the lower hull. The velocity potential may be represented as

$$\phi=\frac{g}{i\omega}\left(\phi_I+\phi_D\right)+\sum_{n=1}^{N}\sum_{j=1}^{\infty} i\omega X_{n,j}\phi_{n,j}, \tag{2.9}$$

where ***g*** is the gravitational acceleration, ϕ_I is the incident wave potential and ϕ_D is the diffraction potential. According to this representation, the linear hull surface conditions for the *n*-th velocity potential may be

$$\frac{\partial}{\partial n}\phi_{n,8j+1}=\begin{cases}\tilde{\psi}_{j+1}(x)n_x & on\,the\,n-th\,and\\ & n'-th\,hull\,surface,\\ 0 & on\,the\,other\,hulls,\end{cases} \tag{2.10}$$

$$\frac{\partial}{\partial n}\phi_{n,8j+2} =\begin{cases}\tilde{\psi}_{j+1}(x)n_x & on\,the\,n-th\ \,hull\,surface,\\ -\tilde{\psi}_{j+1}(x)n_x & on\,the\,n'-th\,hull\,surface,\\ 0 & on\,the\,other\,hulls,\end{cases} \tag{2.11}$$

$$\frac{\partial}{\partial n}\phi_{n,8j+3} =\begin{cases}\psi_{j+1}(x)n_y & on\,the\,n-th\ \,hull\,surface,\\ -\psi_{j+1}(x)n_y & on\,the\,n'-th\,hull\,surface,\\ 0 & on\,the\,other\,hulls,\end{cases} \tag{2.12}$$

$$\frac{\partial}{\partial n}\phi_{n,8j+4}=\begin{cases}\psi_{j+1}(x)n_y & on\,the\,n-th\,and\\ & n'-th\,hull\,surface,\\ 0 & on\,the\,other\,hulls,\end{cases} \tag{2.13}$$

$$\frac{\partial}{\partial n}\phi_{n,8j+5}=\begin{cases}\psi_{j+1}(x)n_z & on\,the\,n-th\,and\\ & n'-th\,hull\,surface,\\ 0 & on\,the\,other\,hulls,\end{cases} \tag{2.14}$$

$$\frac{\partial}{\partial n}\phi_{n,8j+6} =\begin{cases}\psi_{j+1}(x)n_z & on\,the\,n-th\ \,hull\,surface,\\ -\psi_{j+1}(x)n_z & on\,the\,n'-th\,hull\,surface,\\ 0 & on\,the\,other\,hulls,\end{cases} \tag{2.15}$$

$$\frac{\partial}{\partial n}\phi_{n,8j+7}$$

$$=\begin{cases}\tilde{\psi}_{j+1}(x)(yn_z+zn_y) & \text{on the } n-th \text{ hull surface,}\\ -\tilde{\psi}_{j+1}(x)(yn_z+zn_y) & \text{on the } n'-th \text{ hull surface,}\\ 0 & \text{on the other hulls,}\end{cases} \quad (2.16)$$

$$\frac{\partial}{\partial n}\phi_{n,8j+8}$$

$$=\begin{cases}\tilde{\psi}_{j+1}(x)(yn_z+zn_y) & \text{on the } n-th \text{ and}\\ & n'-th \text{ hull surface,}\\ 0 & \text{on the other hulls,}\end{cases} \quad (2.17)$$

where, $n' = 2N+1-n$, $\partial/\partial n$ denotes the partial derivation with respect to the normal direction to the hull surface, (n_x, n_y, n_z) is components of the normal vector.

Velocity potentials are obtained by means of the three-dimensional boundary element method with the linear free surface Green function [4]. The radiation forces and the diffraction forces are obtained by integrating the velocity potential on the hull surface. Using the radiation forces and the diffraction forces, we obtain the equations of motions of the *n*-th hull. However, it is lengthy to show all equations of motions here. Thus, only the equations of motions in the longitudinal direction are shown here. The equations are categorized into two groups and the symmetric motion is represented as

$$-\left(\omega^2 M_h + \left(\frac{k\pi}{L}\right)^2 AE_x L\right) X_{n,8k+1} \quad (2.18)$$

$$-\omega^2 \sum_{m=1}^{N}\sum_{j=0}^{\infty}\sum_{\ell=1}^{3} AS_{m,n,k+1,8j+2\ell-1} X_{m,8j+2\ell-1}$$

$$=\frac{1}{2}\sum_{m=1}^{2M}\left(f_{h,m,n,1}+f_{h,m,n',1}\right)\tilde{\psi}_{k+1}(x_m)+gE_{n,8k+1}, \quad (2.19)$$

where $k = 0,1,2,\cdots$, $n = 1,2,3,\cdots$, $n' = 2N+1 \quad n$, x_m is the longitudinal position of the center of the column, M_h is the mass of the n-th lower hull and AE_x is the rigidity of the longitudinal direction of the lower hull. Similarly, the equation of anti-symmetric motion is given as

$$-\left(\omega^2 M_h + \left(\frac{k\pi}{L}\right)^2 AE_x L\right) X_{n,8k+2} \quad (2.20)$$

$$-\omega^2 \sum_{m=1}^{N}\sum_{j=0}^{\infty}\sum_{\ell=1}^{3} AS_{m,n,k+1,8j+2\ell} X_{m,8j+2\ell}$$

$$=\frac{1}{2}\sum_{m=1}^{2M}\left(f_{h,m,n,1}-f_{h,m,n',1}\right)\tilde{\psi}_{k+1}(x_m)+gE_{n,8k+2}, \quad (2.21)$$

where the radiation coefficient for the longitudinal direction $AS_{m,n,k,j}$ is defined as

$$AS_{m,n,k,8j+\ell}$$

$$=\begin{cases}0 & \text{when } k \text{ and } j \text{ are even number}\\ & \text{or } k \text{ and } j \text{ are odd number,}\\ 2\rho\int_{S_h}\tilde{\psi}_k(x)\phi_{m,8j+\ell}\, n_x dS & \text{other cases,}\end{cases} \quad (2.22)$$

where S_h denotes the surface of the n-th lower hull.

B. Elastic motion of the upper deck

On the other hand, elastic motion of the upper deck is represented by Green functions. Elastic motions of the deck in $x-y$ plane are represented by Green functions $g_u(x,y,x',y')$ and $g_v(x,y,x',y')$ which satisfy equations of vibration in $x-y$ plane

$$-\omega^2 m_d g_u + G\bar{t}\left\{\left(\frac{\partial^2}{\partial x^2}+\frac{\partial^2}{\partial y^2}\right)g_u + \frac{1+v}{1-v}\left(\frac{\partial^2}{\partial x^2}g_u + \frac{\partial^2}{\partial x\partial y}g_v\right)\right\}$$
$$=\delta(x-x')\delta(y-y'), \quad (2.23)$$

$$-\omega^2 m_d g_v + G\bar{t}\left\{\left(\frac{\partial^2}{\partial x^2}+\frac{\partial^2}{\partial y^2}\right)g_v + \frac{1+v}{1-v}\left(\frac{\partial^2}{\partial y^2}g_v + \frac{\partial^2}{\partial x\partial y}g_u\right)\right\}$$
$$=\delta(x-x')\delta(y-y'), \quad (2.24)$$

where m_d is the unit mass of the upper deck, G is the modulus of torsion, $\bar{t}$ is the equivalent thickness of the upper deck and v is Poisson's ratio. g_u and g_v are obtained by means of the energy method with the free-free boundary condition. The elastic vibration of the upper deck in z direction is represented by a Green function $g_w(x,y,x',y')$ which is presented by Eatock Taylor and Ohkus [2]. It satisfies the equation of the vibration of the thin elastic plate:

$$\left[-\omega^2 m_d + D\left(\frac{\partial^2}{\partial x^2}+\frac{\partial^2}{\partial y^2}\right)\right]g_w = \delta(x-x')\delta(y-y'),$$

(2.25)

where D denotes the flexural rigidity of the upper deck.

Using these Green functions, deformation of the deck is represented as linear summation of the inner forces acting at connection points of columns:

$$d_{m,n,i} = \sum_{k=1}^{2M}\sum_{\ell=1}^{2N}\sum_{j=1}^{6} f_{d,k,\ell,j} G_{i,j}(x_m, y_n, x_k, y_\ell), \quad (2.26)$$

where $d_{m,n,i,j}$ is the deformation of the deck at the point (x_m, y_n) (where the m,n-th column is located), $f_{d,k,\ell,j}$ is the j-th internal force at the $k,\ell-th$ column and $G_{i,j}$ is the Green function for the elastic deformation of the deck. It is noted that $G_{i,j}$ is the general notation of g_u, g_v and g_w, and it also represents gradients of g_u, g_v and g_w.

(2.26) is transformed to represent the displacement of the lower hull $h_{m,n,i}$ at the base of the m, n-th column as a linear summation of internal forces acting on the lower hull

$$h_{m,n,i} = -\sum_{k=1}^{2M}\sum_{\ell=1}^{2N}\sum_{j=1}^{6}\begin{pmatrix} f_{d,k,\ell,j}+ \\ \varepsilon_j f_{h,k,\ell,6-j}\end{pmatrix}\begin{pmatrix} G_{i,j}(x_m,y_n,x_k,y_\ell)+ \\ \varepsilon_{6-j}G_{i,6-j}(x_m,y_n,x_k,y_\ell)\end{pmatrix}, \quad (2.27)$$

where

$$\varepsilon = \begin{cases} h_d & when\ j=4, \\ -h_d & when\ j=5, \\ 0 & other\ case. \end{cases} \quad (2.28)$$

The displacement of the lower hull has a relationship with the deformation of the lower hull

$$h_{m,n,i} = \xi_{n,i}(x_m), \quad i = 1 \sim 4, \quad (2.29)$$

$$h_{m,n,5} = \frac{\partial}{\partial x}\xi_{n,3}(x_m)\ and\ h_{m,n,6} = \frac{\partial}{\partial x} = \xi_{n,2}(x_m). \quad (2.30)$$

Combining these equations, we obtain the final solution.

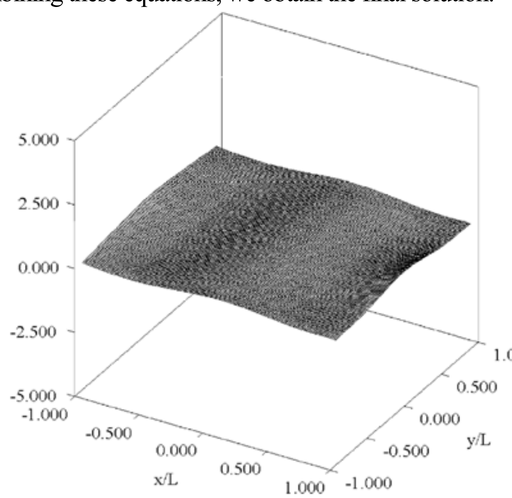

$(a)\chi = 0°$

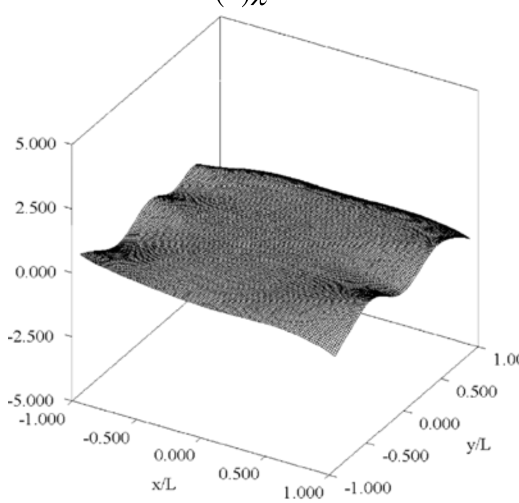

$(b)\chi = 45°$

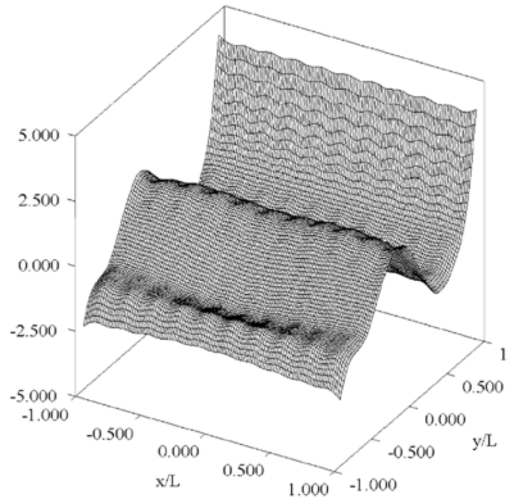

$(c) = 90°$

Fig.2. Snapshots of the upper deck motion for a variation of incident angle.

Fig.2 shows the elastic motion of the upper deck for a variation of the incident angle, where the non-dimensional frequency $\sigma = \omega b^2\sqrt{m_d / D} = 445.0$. The contour represents a snapshot of the elastic motion. It seems that the upper deck motion is large in the beam sea. This fact suggests needs of an anti-motion device or a sophisticated navigation.

III. TWO-DIMENSIONAL ANALISYS

In the case of beam sea, the hydroelastic motion of the VLMOS supposed to be estimated by a two-dimensional analysis, in which the elastic motion of the upper deck is represented by the Euler beam theory and the hydro dynamic problem of the lower hull is reduced to be the two-dimensional linear free surface problem. In addition, the wide spacing approximation in which interaction effect of the evanescent waves is ignored, is applicable since the space between two lower hulls is wide enough compared with the diameter of the lower hull. Equations of motion for the n-th lower hull are given as

$$\begin{aligned} &\{-\omega^2(m_{22}+m_h)+i\omega n_{22}\}\xi_2 \\ &+\{-\omega^2(m_{24}+m_h\ell_G)+i\omega n_{24}\}\xi_4 \\ &= e_2\exp[iK\ell_0]\eta_{n+1}^{(-)} - e_2\exp[-iK\ell_0]\eta_{n-1}^{(+)} + f_2^{(n)}, \end{aligned} \quad (3.1)$$

$$\begin{aligned} &\{-\omega^2(m_{33}+m_h)+i\omega n_{33}\}\xi_3 \\ &= e_3\exp[iK\ell_0]\eta_{n+1}^{(-)} + e_3\exp[-iK\ell_0]\eta_{n-1}^{(+)} + f_3^{(n)}, \end{aligned} \quad (3.2)$$

$$\begin{aligned} &\{-\omega^2(m_{24}+m_h\ell_G)+i\omega n_{24}\}\xi_2 \\ &+\{-\omega^2(m_{44}+I_{xx}m_h\ell_G^2)+i\omega n_{44}\}\xi_4 \\ &= e_4\exp[iK\ell_0]\eta_{n+1}^{(-)} - e_4\exp[-iK\ell_0]\eta_{n-1}^{(+)} + f_4^{(n)}, \end{aligned} \quad (3.3)$$

where m_{ij} is the added mass coefficient, n_{ij} is the damping coefficient, ξ_j is amplitude of the j-th motion (2:Sway, 3:Heave, 4:Roll), e_j is the wave exciting force, l_0 is the distance between adjacent two hulls, l_G is the distance between the center of gravity and the origin of the coordinate, $\eta_n^{(+/-)}$ is amplitude of waves traveling from the n-th lower hull in positive/negative direction and $f_i^{(n)}$ is the internal force acting at the connection point with the column.

Employing the wide spacing approximation, the interaction among radiation waves are represented as

$$\eta_n^{(+)} = \xi_2 \overline{A}_2^{(+)} + \xi_3 \overline{A}_3^{(+)} + \frac{B}{2}\xi_4 \overline{A}_4^{(+)} + \eta_{n+1}^{(-)} C_R \exp[iK\ell_0] + \eta_{n-1}^{(+)} C_T \exp[-iK\ell_0], \tag{3.4}$$

$$\eta_n^{(-)} = \xi_2 \overline{A}_2^{(-)} + \xi_3 \overline{A}_3^{(-)} + \frac{B}{2}\xi_4 \overline{A}_4^{(-)} + \eta_{n+1}^{(-)} C_T \exp[iK\ell_0] + \eta_{n-1}^{(+)} C_R \exp[-iK\ell_0], \tag{3.5}$$

where $\overline{A}_j^{(+/-)}$ denotes the ratio between amplitude of the j-th mode and amplitude of the radiation waves to positive/negative direction, C_R is the reflection coefficient and C_T is the transmission coefficient.

Elastic motion of the upper deck is given as a summation of vibrating modes

$$\varsigma(y) = \sum_{j=0}^{\infty} \psi_j(y)\varsigma_j \tag{3.6}$$

where ς_j denotes amplitude of the vibration mode. The equation of vibration of the upper deck is given as

$$\left(-m_d\omega^2 + EI_d p_j^4\right)\varsigma_j = -\frac{1}{b}\sum_{n=1}^{2N}\left[f_3^{(n)}\psi_j(y_n) + \left(f_4^{(n)} - h_d f_2^{(n)}\right)\frac{d}{dy}\psi_j(y_n)\right], \tag{3.7}$$

where EI_d is rigidity of the upper deck and y_n is horizontal position of the lower hull. It is assumed that the upper deck moves as a rigid body in the horizontal plane. Thus, the equation of horizontal motion is given as

$$-m_d b\omega^2 \xi_2 = -\sum_{n=1}^{2N} f_2^{(n)} \tag{3.8}$$

Combining equations (3.1), (3.2),(3.3),(3.4),(3.5),(3.6),(3.7) and (3.8), a system of linear equations is obtained. The solution is obtained by solving this system of linear equations.

Fig.3 shows a comparison between the three-dimensional solution and the two-dimensional solution.

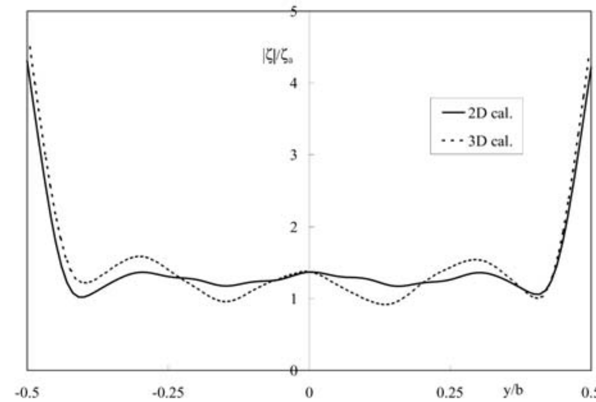

Fig.3. Comparison of amplitude of elastic motion of the upper deck at x=0 between the two-dimensional calculation and the three dimensional calculation. The rigidity of the upper deck is $D = 3.6\times10^9$ Nm ,the incident wavelength is $\lambda/L = 0.1$ and the incident angle $\chi = 90°$.

It seems the two-dimensional calculation is in good agreement with the three-dimensional calculation. We then decided to use two-dimensional calculation for the parametric study of anti-motion device in the next session.

IV. MOTION REDUCTION AND ENERGY ABSORPTION

An attempt for reducing the deformation is considered, that hydraulic pumps are set on the columns and these pump oil into smoothing accumulators which then drain at a constant rate through a hydraulic motor coupled to an electrical generator. In addition, a suspension system is equipped at the column to keep the upper deck at a certain level. This system reduces the deformation and generates electrical power at the same time. In order to determine a performance requirement for the system, a parametric study, in which the system is expressed as a linear spring and damping system, is carried out.

Fig. 4 shows the amplitude of elastic motion of the upper deck at different incident wavelengths, two of which correspond to peaks appearing in a diagram of the motion amplitude of the weather side tip of the upper deck versus the wavelength. The incident wave travels in positive y-direction.

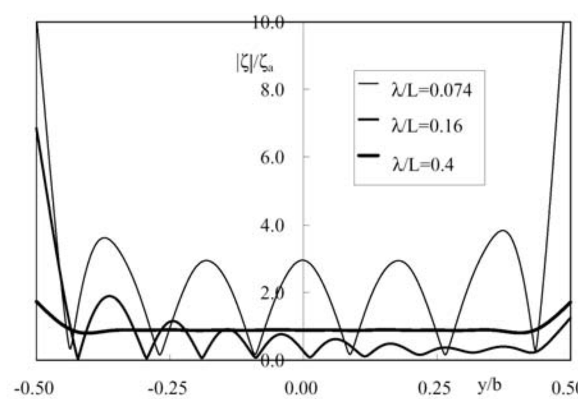

Fig.4 The amplitude of elastic motion of the upper deck

at different incident wave lengths.

The shape of the elastic motion shows that $\lambda/L = 0.074$ corresponds to natural frequency of the six nodes vibration mode of the upper deck and $\lambda/L = 0.16$ corresponds to natural frequency of the heaving motion of the lower hull. It is noted that there is no natural frequency, which corresponds to $\lambda/L = 0.4$, and this wavelength is much longer than the breadth of the lower full. Thus, the motion of the upper deck at this wavelength is very calm and the amplitude ratio of most part is one.

It is supposed that the resonance due to the vibration mode is not serious in practice, because the natural period of the vibration mode is rather short and long crested waves of such a short period does not exist in the real sea. We then decide to reduce the amplitude at the heaving resonance of the lower hull.

We test two different spring stiffness. The weak spring is chosen so that its spring coefficient is 1/100 of the restoring coefficient due to the buoyancy of the lower hull. Fig. 5 shows the amplitude of elastic motion at the weather side edge versus incident wave length for the variation of additional damping coefficient, where n denotes the additional damping coefficient and n_0 denotes the damping coefficient due to the radiation waves of the lower hull at $\lambda/L = 0.16$.

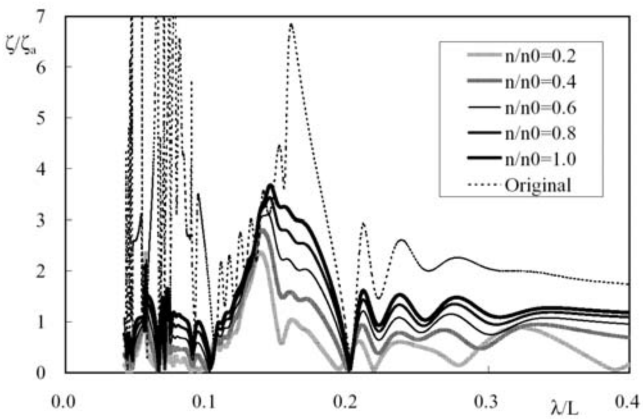

Fig.5 The amplitude of elastic motion at the weather side edge versus incident wave length for the variation of additional damping coefficient. The spring coefficient is 1/100 of the restring coefficient of the lower hull

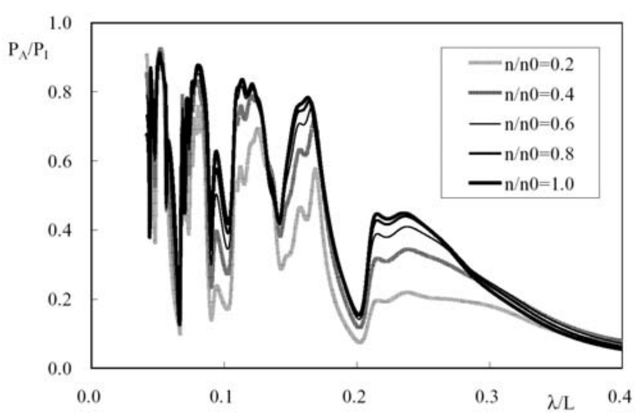

Fig.6 Ratio between the absorbed power and the incident wave power for the variation of additional damping coefficient. The spring coefficient is 1/100 of the restoring coefficient of the lower hull.

The dotted line presents the original amplitude at the weather side edge. It is found that the peak due to the heaving resonance of the lower hull is reduced to 1/2 of the original amplitude. In addition, the amplitude at the short wave range, i.e. $\lambda/L < 0.1$, is significantly reduced and peaks due to the resonance of vibration modes are disappeared. The strength of the additional damping seems important to reduce the amplitude, and the weakest additional damping the best to reduces the amplitude. However, in terms of the wave power absorption, the weak additional damping gets less power as shown in Fig.6.

It is noted that the absorbed power is estimated as the work done by the additional damping, where the efficiency of the electric generator is assumed to be 100 percent. It is interesting that the efficiency of the wave energy absorption at the short wave range is relatively high.

The amplitude of the hard spring case is shown in Fig. 7, although the strength of the spring constant is still 1/10 of the restoring coefficient of the lower hull.

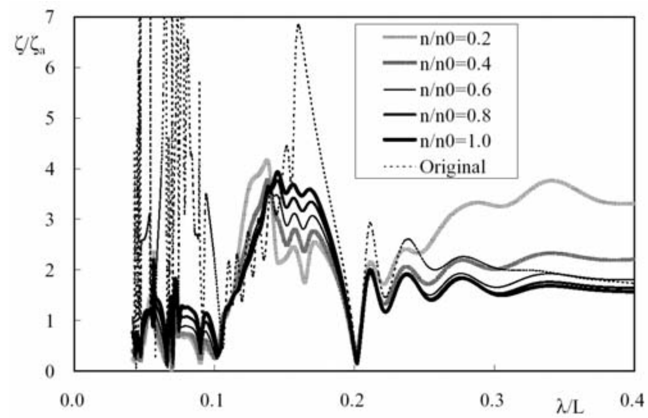

Fig.7 The amplitude of elastic motion at the weather side edge versus incident wave length for the variation of additional damping coefficient. The spring coefficient is 1/10 of the restring coefficient of the lower hull

The reduction of the elastic motion is smaller than that in the case of the weak spring, and the amplitude at the long wavelength range is relatively large, when the additional damping is small. Fig. 8 shows the wave energy absorbing ratio for the case of the strong spring.

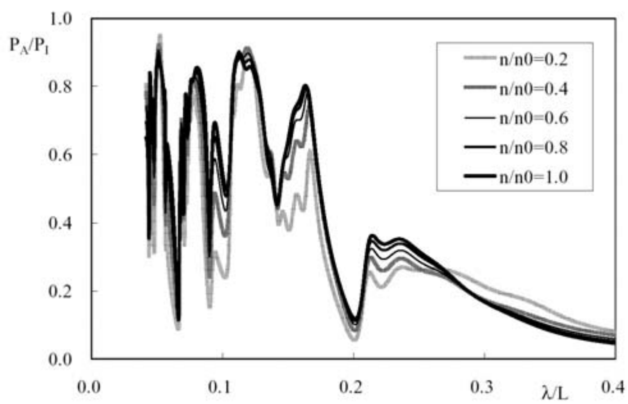

Fig.8 Ratio between the absorbed power and the incident wave power for the variation of additional damping coefficient. The spring coefficient is 1/10 of the restoring coefficient of the lower hull.

The efficiency of the strong spring case is almost the same as that of the weak spring case. However, when the additional damping is small, the efficiency is better than that of the weak spring case with the same damping condition.

Summarizing these results, it is suggested that the weak spring and the weak damping is efficient for reducing the motion of the upper deck and this is not always good for improving the efficiency of the wave energy absorption. It seems impossible to achieve the minimization of motion and the maximizing the wave power absorption at the same time. However, at least, it can be stated that adding the spring and the damping is effective for both the anti-motion and the wave absorption. A problem is how to achieve such a weak spring coefficient with enough stroke, since the spring should support the weight of the upper deck. We need to solve this problem in the future.

V. CONCLUSIONS

The Green function for hydroelastic analysis of vibrating free-free plates is used for representing the elastic motion of the upper deck, and the conventional modal analysis and the three-dimensional boundary element method are employed for hydroelastic analysis of the lower hull. Combining these methods, the hydroelastic behavior of VLMOS in waves is analyzed. An example of the elastic motion of the upper deck is obtained for the case of $\sigma = 445.0$, and the amplitude of elastic motion at the weather side tip of the upper deck is large in the beam sea. We then made an attempt for the reduction of the upper deck motion and absorbing the wave energy at the same time, and analyzed it by the two-dimensional approach. It is found that to achieve the minimization of motion and the maximizing the wave power absorption at the same time seems impossible. However, at least, it can be stated that adding the spring and the damping is effective for both the anti-motion and the wave absorption.

References

[1] K. Takagi, K. Yamamoto, M. Kondo, T. Funaki, and Z. Kawasaki, "Conceptual Design of a Very Large Mobile Structure for the Renewable Energy Plant" Proceedings of the Asia Pacific Workshop on Marine Hydrodynamics, Kobe, 2002, pp.239-244.

[2] R. Eatock Taylor, and M. Ohkus, "Green Functions for Hydroelastic Analysis of Vibrating Free-Free Beam and Plate" J Applied Ocean Research, vol. 22, 2000, pp.295-314.

[3] K. Takagi, and W. Yano, "Analysis of Hydroelastic Behavior of a Very Large Mobile Offshore Structure in Waves." Proc. of IWWWFB, Le Croisic, France, 2003.

[4] Kashiwagi et. al, "Hydrodinamics for floating bodies."Seizando,2003.